一般講演
資源開発技術・岩盤工学
2018年3月28日(水) 09:00 ～ 11:45 第2会場 (3号館3F, 33号講義室)

[2201-10-04] Transient Stress Disturbances Induced Change in Permeability of Kushiro Cretaceous Sandstone

Transient Stress Disturbances Induced Change in Permeability of Kushiro Cretaceous Sandstone

〇Sophea BOEUT[1]、OSHIMA Teppei [1]、FUJII Yoshiaki [1]、KODAMA Jun-ichi [1]、 FUKUDA Daisuke[1]、MATSUMOTO Hiroyuki [2]、 UCHIDA Kazumi[2] （1. Hokkaido University、2. Kushiro Coal Mine）
〇Sophea BOEUT[1], Teppei OSHIMA[1], Yoshiaki FUJII[1], Jun-ichi KODAMA[1], Daisuke FUKUDA[1], Hiroyuki MATSUMOTO[2], Kazumi UCHIDA[2] （1. Hokkaido University, 2. Kushiro Coal Mine）

キーワード：Transient stress disturbances、Axial stress、Pore pressure、Permeability、Kushiro Cretaceous sandstone
Transient stress disturbances, Axial stress, Pore pressure, Permeability, Kushiro Cretaceous sandstone

These phenomena might be induced by change in transient stress disturbances from these etc. in paperback the change in permeability of Kushiro Cretaceous sandstone by transient stress disturbances which change might be potentially used for the enhanced methane gas recovery at Kushiro Coal Mine. The saturated specimens with the dimension of 30 mm in diameter and 60 mm in length under triaxial compression to the axial stress or pore pressure disturbances.Under axial stress disturbance amplitudes of 0-11 MPa and confining pressure of 3-15 MPa, The permeability of the specimens decreased by the disturbances for both pre-post-failure, the reduction amount is greater than was with a greater than confidence pressure but kept almost constant with stress disturbance amplitudes.Under pore pressure disturbance amplitudes of 1.8 MPa and confining pressure of 10 MPa, the permeability of the intact specimen increased by the disturbance and continued increasing by failure, though it decreased by disturbances for the post-failure regime. by the transient pore pressure disturbances inducing microcracks, unclogging the micro-pathway, etc. This increase may be caused by the enhanced methane gas recovery.This increase may be caused by the enhanced methane gas recovery.This increase may be caused by the enhanced methane gas recovery.

1. Introduction

Seismic waves caused by earthquakes or human activity may change the underground property. For examples, seismic waves resulted in the change in the level (Beresnev & Johnson, 1994; Manga et al., 2012) and the temperature (Mogi et al., 1989) of the ground water or the petroleum production (Beresnev & Johnson, 1994). It was reported that during the 1950s and 1960s, when the underground nuclear explosion tests were carried out by the Union of Soviet Socialist Republic and the US, there occurred fewer earthquakes more than M8.0 (Fujii et al., 2017). The causes of the above phenomena might be the change in rock permeability by the transient stress disturbances due to the creation of microcracks, clearing the mineral particles clogged the pore spaces of the pathways, etc. (Manga et al., 2012). The change in permeability of intact and triaxially fractured rocks by transient stress disturbances were therefore investigated. The fortunate increase in permeability by the transient disturbances may encourage its utilization to enhance gas recovery, prevent the future large earthquakes by inducing small earthquakes, and de-route the underground water flow for various purposes.

2. Rock sample and experimental procedure

The core specimens were provided from Kushiro Coal Mine located in eastern Hokkaido along the Pacific Ocean. The cores were drilled from Cretaceous sandstone layer, where the methane gas has been extracted, underlying the Paleogene coal bearing formations through the borehole No. 72, in the depths of 322.65 to 323.50 m, the second drilling pit at the inclined shaft 650 m from the entrance (Boeut et al., 2017). Under microscopic analysis, the rock is wacke fine-grained sandstone, composed mainly of quartz and plagioclases. The matrix is muddy and mainly consists of smectite (Fig. 1).

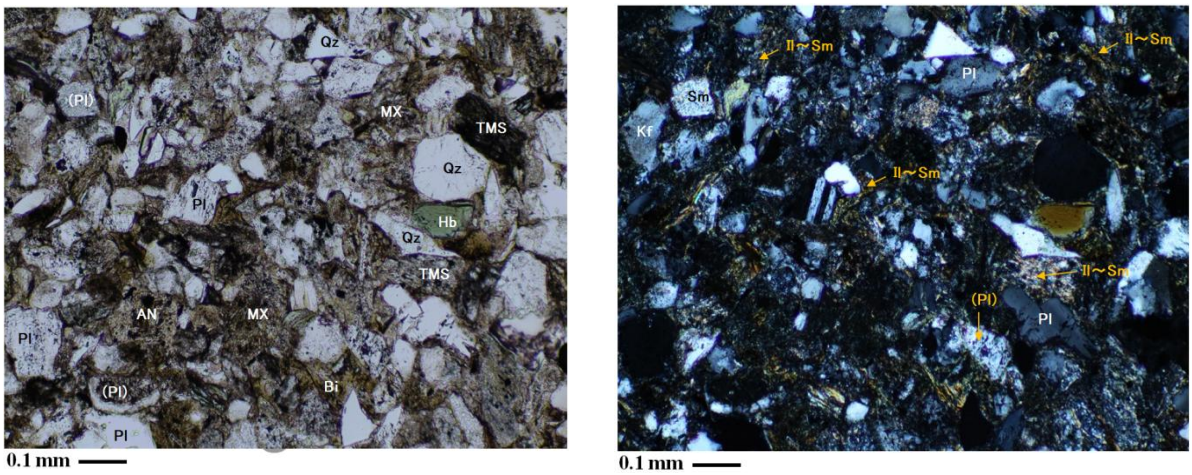

(a) Open Nicol (b) Crossed Nicols

Fig.1 Microscope image of Kushiro Cretaceous specimen, (Qz: quartz, Pl: plagioclases, Mx: matrix, Sm: smectite, Kf: potash feldspar, Bi: biotite, Hb: ordinary amphibole, AN: andesite, Il: illite, TMS: transformed mudstone).

The cylindrical specimen with diameter of 30 mm and length of 60 mm was vacuum saturated with pure water and connected to a pair of strainless steel endpieces, each with a hole at the center where pore water can pass through. The silicon sealant was applied to the specimen side to maintain the water flow within the specimen. A heat-shrinkable tube was used to jacket the endpiece-attached specimen to prevent the direct contact of the confining fluid with the specimen. The specimen was vacuum saturated again and inserted into the ultra-compact triaxial cell (Alam et al., 2014). The specimen was subjected to the axial stress or pore pressure disturbances before and after the triaxial compression.

In terms of the axial stress disturbance, pore pressure of 1 MPa was subjected at the bottom of the specimen and the upper end was open to the atmospheric pressure (Fig. 2) after the confining pressure of 3, 10 or 15 MPa was applied. The axial stress disturbance

was applied under the frequency of 0.5 Hz in 200 seconds. For pore pressure disturbance, the same condition of pore pressure was brought into operation, and the experiment was under confining pressure of 10 MPa. The pore pressure disturbance amplitudes were between 1.0 and 1.8 MPa with the frequency of 0.1 Hz in 200 seconds. The detail of the experimental condition for each specimen was illustrated in Table 1. Experimental procedure is as follows (Fig.3). (1) The intact specimen was kept under constant hydrostatic pressure for 24 hours. (2) The axial stress or pore pressure disturbance was applied. (3) The specimen was returned to the constant hydrostatic pressure state for 24 hours. (4) The axial compression was conducted at the constant rate of 10^{-5} s^{-1} (0.036 mm/min) until the residual strength state was confirmed. Steps (1) to (3) were repeated for the fractured specimen.

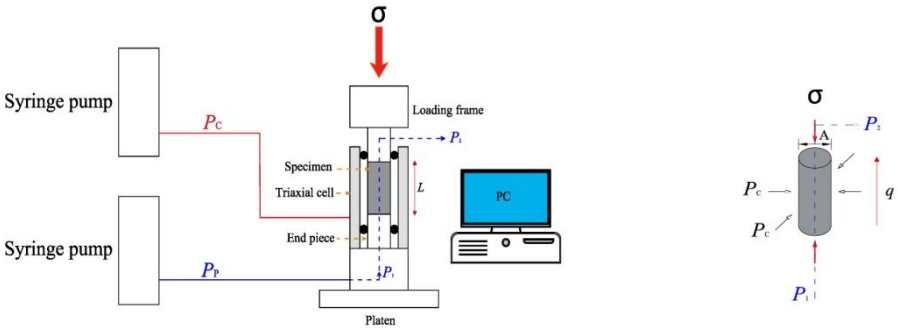

(a) Experimental apparatus (b) Stress state inside the specimen

Fig. 2 The permeability measurement apparatus.

The permeability of the intact rock during 24-hour-constant hydraulic pressures k_1 before transient stress disturbance, and k_2 after the disturbance, were measured by the constant head method. After the triaxial compression was applied, the permeability of the fractured rock before and after the transient stress disturbance were measured as k_3 and k_4, respectively. The calculation of the permeability was based on the change in water volume in the syringe plump as:

$$k = \frac{q\mu}{A}\left(\frac{\mathrm{d}p}{\mathrm{d}x}\right)^{-1} \qquad \text{(eq. 1)}$$

where k (m^2) is the permeability, q is the flow rate (m^3/s), μ is the fluid viscosity (Pa·s), A is the cross-sectional area (m^2) of the specimen, and dp/dx is the pressure gradient (Pa/m). The viscosity of water (μ) is 9.57 x 10^{-4} (Pa·s) at 295 K.

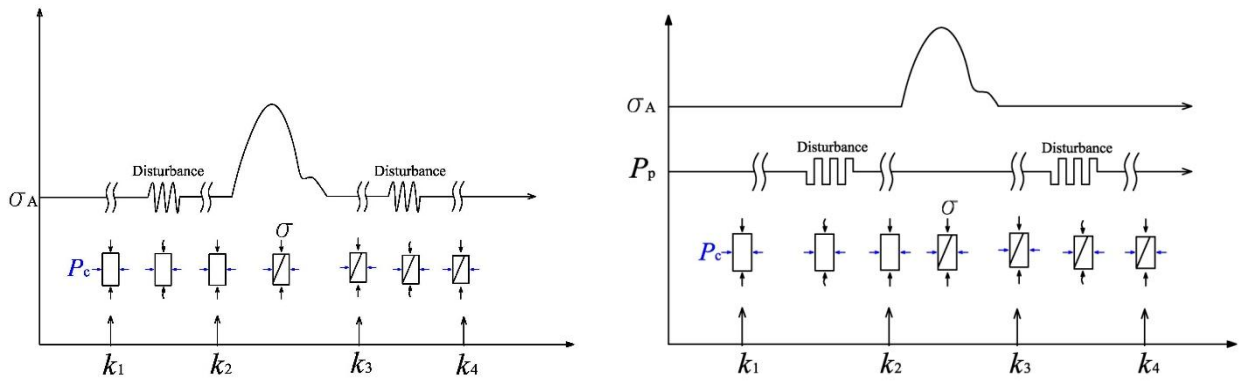

(a) Axial stress disturbance (b) Pore pressure disturbance

Fig. 3 Experimental procedure.

Table 1: The experimental conditions. AS-KCS: Axial stress disturbance on Kushiro Cretaceous sandstone. P_P-KCS: Pore pressure disturbance on Kushiro Cretaceous sandstone. AS-KCS12: Axial stress disturbance on Kushiro Cretaceous sandstone for an experiment of 264 hours. Temperature was kept constant at 295 K.

Axial stress disturbance			Pore pressure disturbance		
ID	P_C (MPa)	$\Delta\sigma_A$ (MPa)	ID	P_C (MPa)	ΔP_P (MPa)
AS-KCS1	3	1	P_P-KCS1	10	1.8
AS-KCS2	10	0	P_P-KCS2		1.4
AS-KCS3		1	P_P-KCS3		1.0
AS-KCS4		3			
AS-KCS5		4			
AS-KCS6		5			
AS-KCS7		7			
AS-KCS8		9			
AS-KCS9		11			
AS-KCS10	15	1			
AS-KCS11		3			
AS-KCS12	10	5			

3. Results and discussions

3.1 Axial stress disturbance

The permeability tended to decrease due to the axial stress disturbances for either pre- or post-failure, yet it increased by failure (Fig. 4). The permeability continued to decrease with time in the 264-hour test (Fig. 4b). And also greater amount of decrease in permeability was observed with the increase of the confining pressure (Fig. 5a). Therefore, the decrease can be basically explained by the consolidation for pre-failure rock. The decrease amount was not affected by the stress disturbance amplitude (Fig. 5b).

In contrast, the amount of change in permeability demonstrated constant with confining pressure (Fig. 5c) though the permeability decreased more with the axial stress disturbance amplitudes (Fig. 5d) for post-failure specimen. This provided the information that the axial stress disturbance caused decrease in permeability for fractured rock. The stress disturbance may enhance either closure of the rupture planes or producing the gouge (Fig. 8) along the planes to block the points of the narrowest aperture (Liu & Manga, 2009).

3.2 Pore pressure disturbance

Under confining pressure of 10 MPa, the specimens were experimented with different values of pore pressure disturbances. The permeability decreased by pore pressure disturbances except for pre-failure of Pp-KCS1 (Fig. 6). However, the permeability of pre-failure specimen kept rising up with the increase in pore pressure disturbance amplitude until it moved greater than the reference line of permeability (k_{ref}), which meant the permeability increased (Fig. 7a). This increase would be due to the pore pressure disturbance which created the micro-pathways, or unclogged the existing micro-pathways (Beresnev et al., 2011, Elkhoury et al., 2006, Manga et al., 2012) and experimentally support the seismic EOR (Enhance Oil Recovery) technique (Pride et al., 2008).

At the lowest disturbance amplitude, the permeability of post-failure rock was slightly below the reference permeability (k_{ref}). The permeability presented a drop with the larger pore pressure disturbance amplitudes (Fig. 7b). The enhancement of closure of the rupture planes (Fig. 8) by the pore pressure disturbance would be the foremost cause of the decrease in permeability for the

post-failure specimens.

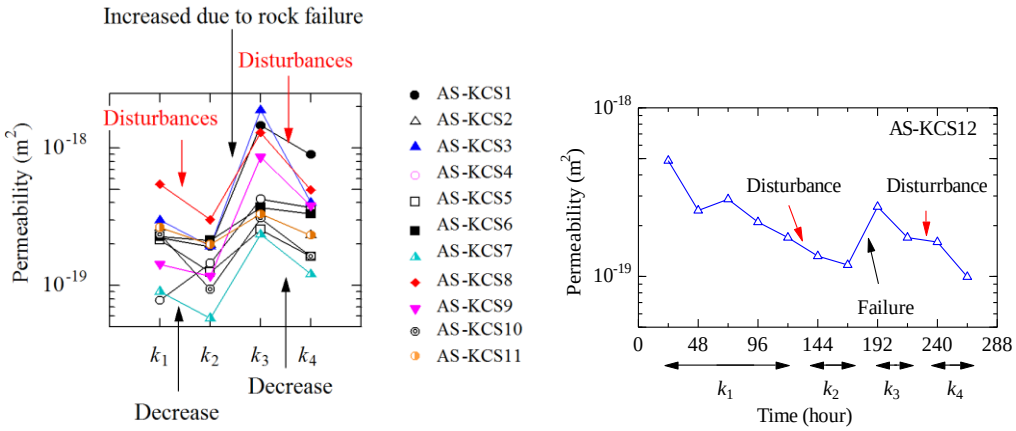

(a) Experiment with 24-hour loop

(b) The 264-hour test

Fig. 4 Change in permeability due to stress disturbances and triaxial compression.

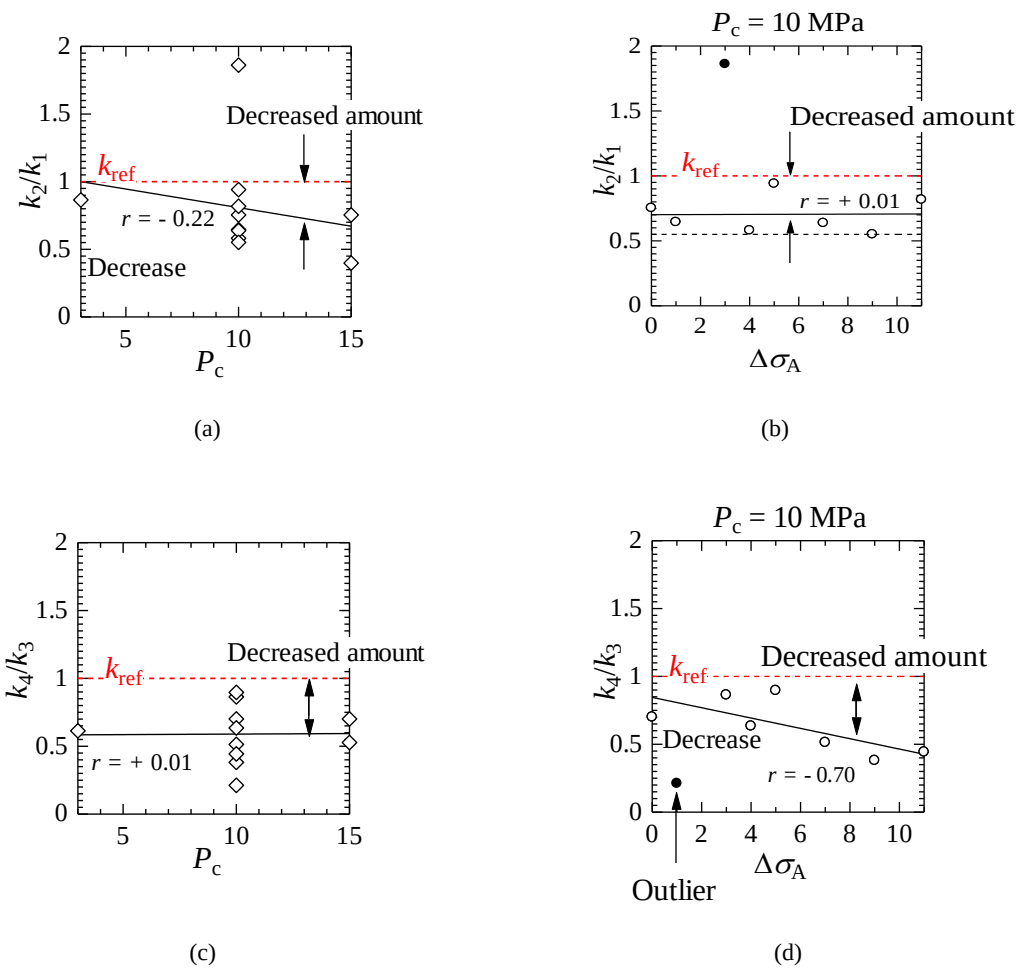

Fig. 5 (a) and (c): Change in permeability vs. confining pressure of pre-failure and post-failure stages respectively. (b) and (d): Change in permeability vs. axial stress disturbances of pre-failure and post-failure stages respectively for P_C =10 (MPa). The outlier data shown as solid circles in (b) and (d) are ignored. k_{ref} is the ratio of 1.0 as the reference permeability.

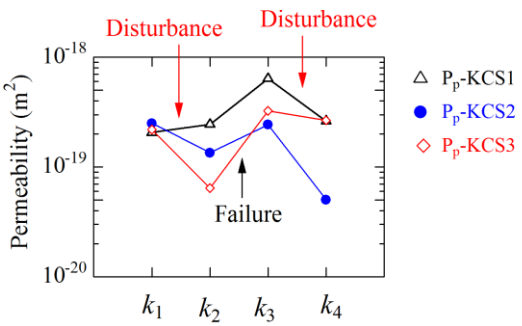

Fig. 6 Permeability change due to pore pressure disturbance and triaxial compression under confining pressure of 10 MPa.

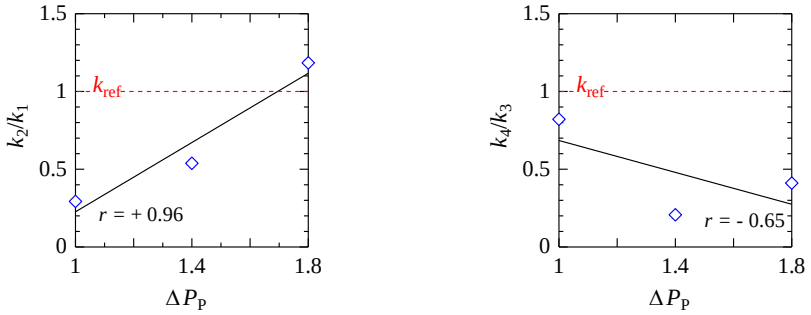

(a) (b)

Fig.7 Change in permeability vs. pore pressure disturbance amplitude for (a) of pre-failure, and (b) post-failure stages respectively. k_{ref} is the ratio of 1.0 as the reference permeability.

(a) (b)

Fig. 8 The specimen (P_P-KCS3) after experiment: (a) specimen with rupture planes, and (b) the gouge along the rupture planes.

4. Concluding remarks

The permeability of Kushiro Cretaceous sandstone under triaxial compression was measured with the transient axial and pore pressure disturbances under various confining pressures. The permeability of the Cretaceous sandstone decreased by the axial stress disturbance although it increased by rock failure. The amount of decrease in permeability of pre-failure sandstone was greater with confining pressure; however, there was no effect from the axial stress disturbance. In spite of that, the amount of decrease in permeability for post-failure rock had no effect of confining pressure, but it became greater with the axial stress disturbance. The permeability of the higher-pore pressure disturbance was found to increase due to the pore pressure disturbance for pre-failure rock, but, for post-failure rock, the disturbance caused the decrease in permeability. Further investigation on the effect of pore pressure disturbance on the permeability and the mechanism of the changes in permeability would be needed.

Acknowledgement

The authors gratefully acknowledge Kushiro Coal Mine for their kind cooperation and rock samples providing for this study. The research is funded by JICA under AUN/SEED-Net program (J16-10145).

References

Alam, A. B., Niioka, M., Fujii, Y., Fukuda, D. & Kodama, J. (2014). Effects of confining pressure on the permeability of three rock types under compression. Int. J. Rock Mech Min Sci, 65, pp. 49-61.

Beresnev, I. A, Gaul, W., and Vigil, R. D. (2011). Direct pore-level observation of permeability increase in two-phase flow by shaking. Geophys. Res. Lett., 38, L20302, doi:10.1029/2011GL048840.

Beresnev, I. A. & Johnson, P. A. (1994). Elastic-wave stimulation of oil production: A review of methods and results. Geophysics, 59, pp. 1000-1017.

Boeut, S., Oshima, T., Fujii, Y., Kodama, J., Fukuda, D., Matsumoto, H. & Uchida, K. (2017). Impact on permeability due to axial stress disturbances for cretaceous sandy shale. Proc. Fall Meeting of MMIJ, PY2-73.

Elkhoury, J. E., Brodsky, E. E., & Agnew, D. C. (2006). Seismic waves increase permeability. Nature, 441, pp. 1135-1138, doi:10.1038/nature04798

Fujii. Y, Yamada. M, Fukuda. D & Kodama. J. (2017). Prevention of giant earthquakes by underground nuclear explosions, Proc. Spring Meeting of MMIJ, #3411.

Liu, W. & Manga, M. (2009). Changes in permeability caused by dynamic stresses in fractured sandstone. Geophys. Res. Let., 36, L20307.

Manga, M., Beresnev, I., Brodsky, E. E., Elkhoury, J. E., Elsworth, D., Ingebritsen, S. E., Mays, D. C. and Wang, C.-Y. (2012), Changes in permeability caused by transient stresses: Field observations, experiments, and mechanisms, Rev. Geophys., 50, RG2004, doi:10.1029/2011RG000382.

Mogi, K., Mochizuki, H. & Kurokawa, Y. (1989). Temperature changes in an artesian spring at Usami in the Izu Peninsula (Japan) and their relation to earthquakes. Tectonophysics, 159 (1-2), pp. 95-108.

Pride, S. R., Flekkøy, E. G., & Aursjø, O. (2008), Seismic stimulation for enhanced oil recovery, Geophysics, 73 (5), pp. 023-035.